The International Innovations Journal of Applied Science (IIJAS) Vol. 1, No.2, 15-09-2024
المجلد الأول العدد الثاني 15-9-2024 (IIJAS) مجلة ابتكارات الدولية للعلوم التطبيقية
https://doi.org/10.61856/wb55x818

SCIENTIFIC EVENTS GATE

The International Innovations Journal of Applied Science

Journal homepage: https://iijas.eventsgate.org/iijas

ISSN: 3009-1853 Online

Physical properties and microstructural corrosion properties of Laser-bent 304 Stainless Steel Sheets

Mastura A Abdalshafie Efhema

University of Manchester, Manchester, United Kingdom

ARTICLE INFO

Article history:
Received 14 Mar. 2024,
Revised 19 May 2024,
Accepted 29 May 2024,
Available online 15 Sep. 2024

Keywords:
Martials laser treatment
Laser bending
304 stainless steels
Sensitization

ABSTRACT

Laser treatment by laser bending is a technique of treating sheet metal by thermal residual stresses generated by laser assisted heating without any externally applied mechanical forces. The advantages of laser assisted bending over conventional bending include flexibility of non-contact processing, amenability to materials with diverse shape/geometry, and high precision/productivity. Up to now, most of previous work on laser bending was concentrated on study of bending angles/shapes with laser operating conditions, and modelling of the thermal process, however, no work has been reported on corrosion behavior of the laser-bended components. Since the laser bending is a thermal process, it is believed that the thermal process could not only alter microstructure, but also affect corrosion performances, such as intergranular corrosion, due to possible sensitisation caused by repeating laser scans. The aim of the present work is to investigate corrosion performance of laser-bent 304 austenitic-steel sheet with thicknesses of 2 mm and 1.5 mm, respectively, using a 2 kW CO_2 laser. After laser treatment, the laser-bent samples were characterised in terms of microstructural change within bent zones consisting of melt-zone and heat-affected zone, using optical microscopy and scanning electron microscopy (SEM). Hardness profiles were obtained across the bent zones. Corrosion performances of the laser-bent evaluated by means of electrolytic etching in oxalic acid and double-loop electrochemical potentiokinetic reactivation (DL-EPR) tests. Laser bending is a thermal process, it is believed that the thermal process could not only alter microstructure, but also affect corrosion performances, due to possible sensitisation caused by repeating laser scans.

1. Introduction

Laser bending is a technique of modifying the curvature of sheet metal by thermal residual stresses generated by laser assisted heating without any externally applied mechanical forces. The advantages of laser assisted bending over conventional bending include flexibility of non-contact processing, amenability to materials with diverse shape/geometry, and high precision/productivity. Up to now, most of previous work on laser bending has been concentrated on study of bending angles/shapes with laser operating conditions, modelling of the thermal process and microstructural evolution (H. Shen *et al.* 2006, B.S. Yilbas *et al.* 2012). In the field of laser bending and forming of metallic sheets, a number of studies have been conducted by various researchers to explore the underlying mechanisms and analyse the thermal stress involved in the process. Notable among these studies are the works by (Yilbas et al. 2012, 2014) on laser

* Corresponding author.
E-mail address: Abdoalshafie_mastura@yahoo.com

https://doi.org/10.61856/wb55x818

bending of AISI 304 steel sheets and (Shen et al. 2006, 2010) who developed an analytical formula for estimating deformation in laser forming and conducted an experimental study on negative laser bending process of steel foils, respectively. (Yongjun Shi et al. 2012) also investigated the effect of different heating methods on deformation of metal plate under upsetting mechanism in laser forming. Additionally, other significant studies in this area include the research on the mechanisms of laser forming for the metal plate by (Yau et al. 2006), laser forming of open-cell aluminium foams by (Quadrini et al. 2010), and laser bending of lead frame materials by (Shi et al. 1998), and the investigation of underwater pulsed laser forming by (Y. Shi *et al.* 2014). However, the laser-bent components are believed that the thermal process could not only alter microstructure, but also increase the susceptibility to intergranular corrosion due to possible sensitisation caused by repeating laser scans. This paper presents a study of microstructural and corrosion characterization of laser-bent of stainless steel, including 304. Various relations between bend angle, microstructure, microhardness and corrosion performance with laser operating conditions have been established. In this study, the laser bending process of 304 austenitic stainless steel was investigated, focusing on bending angle, microstructure, microhardness, and corrosion performance within the bent zone and heat-affected zones (HAZs). The bending angle was found to vary from 6.5° to 29.5° for 304 stainless steel, with the angle increasing as scanning velocity decreased and the number of passes increased. However, achieving larger bending angles necessitates surface melting. The microstructure of the bent zone comprised a melt zone with a significantly refined dendritic structure, followed by HAZ (I) characterized by coarsened grains, and then HAZ (II) exhibiting pronounced grain elongation. The microhardness variation, as measured by Vickers hardness profiles across the specimen's thickness, demonstrated specific patterns corresponding to the different zones.

2. Methodology

2.1. Experimental procedure

2.2 Materials and laser processing

The chemical compositions of ALSI 304 austenitic stainless steels used in this study are given in table 1. Alloy of 304 was received after solution treatment. Laser bending was carried out using a 2 kW CO_2 laser with Gaussian beam profile under Air shrouding environment to minimise oxidation. The dimension of this alloy is 100 mm x 30 mm with thickness of 2 mm and 1.5mm. One end of the sheet was clamped in a fixture to remain the length of the sheet to be 90 mm. Laser beam is uniform across the width of the specimen (the x-direction) in figure 1 and 2. In addition the laser operating conditions are shown in table 2.

2.3 Materials characterisation

Microstructures of the alloys were examined after electro-etching in 10% oxalic acid at a current density of 1 A/cm^2 using optical microscopy and scanning electron microscopy (SEM). Microhardness crosses the different regions of laser–bent specimens was measured by a Vickers microhardness tester (Y. Shi *et al.* 2014).

https://doi.org/10.61856/wb55x818

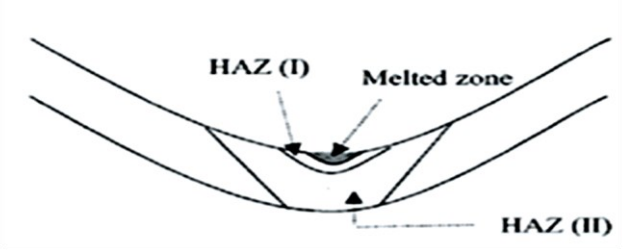

Figure 1. Schematic of laser bending process.

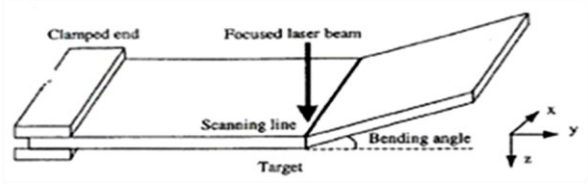

Figure 2. Schematic diagram of atypical bent zone.

Table 1: Chemical composition of the materials used in the experiments, wt.

Alloy	C	Mn	P	S	Si	Cr	Ni	Fe
304	0.04	2.00	0.045	0.03	1.00	19.00	9.25	Bal.

Table 2: Summery of the laser operating condition and parameter employed in laser bending of AlSI 304 stainless steel.

Work piece thickness (mm)	Work piece width (cm)	Work piece length (cm)	Laser power (W)	Processing Velocity (V) (mm/min)	Passes Number (N)	Laser Spot diameter(D) (mm)
2	3	10	300-400	5-40	5-40	3

3. Corrosion test

The freshly polished specimens using 1µm was found that the laser operating conditions were controllable to avoid melting of the top surface (B.S. Yilbas *et al.* 2014, F. Quadrini *et al.* 2010), but when larger bending angles were produced, a small degree of melting became inevitable, figure 3, shows variation of bending angles with laser operating conditions for 304 alloy, with indication of non-melting or melting occurred during laser bending. Under the laser diamond paste were etched in10% oxalic acid at 1A/cm^2 for 90 s according to ASTM A262. Then the etched surface was examined on a metallographic microscope.

3.1 Results and discussion

3.1.1 Bending angles

The relationships indicate that bending angle increased with decrease in scanning velocity and increase in number of scans (N). It was found that the laser operating conditions were controllable to avoid melting of the top surface ((B.S. Yilbas *et al*. 2014, F. Quadrini *et*

https://doi.org/10.61856/wb55x818

al. 2010), but when larger bending angles were produced, a small degree of melting became inevitable, figure 3, shows variation of bending angles with laser operating conditions for 304 alloy, with indication of non-melting or melting occurred during laser bending. Under the laser power and beam size applied in the present work, maximum bending angle of 304-g-8 (304 S.S with graven coating samples) was achieved without melting taking place (C.L. Yau *et al.* 2006, H. Shen *et al.* 2010).

scanning velocity on the bending angles.

3.2 Microstructural characteristics and hardness profiles

3.2.1 Microstructural characteristics

Schematic diagram of a typical cross-section of laser-bent specimens was shown in figure 1 and 2. HAZ (I) was defined as experienced by the temperature range between melting temperature and 900 ^{0}C in which chrominium-rich carbides are unlikely to be formed; HAZ (II) by the temperature range

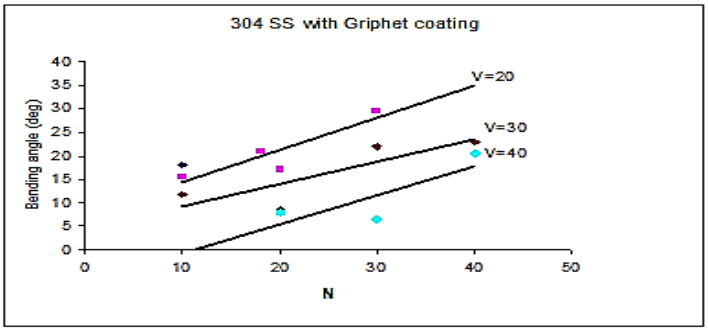

Figure 3. Shows variation of bending angles of 304-g S.S with laser operating condition of laser scans velocity (v) and the number of this scans (N).

From Figure 3, it can be also seen that the bending angle increased continuously as the surface experienced over the melting, which is consistent with the finding reported in (1) describing that the bending angle increased continuously as the laser energy is increased over the melting threshold value, due to insignificant change of total residual strain across the melting threshold. The variation of corrosion behaviour within the HAZs and BZs with laser operating conditions for 304 sheets with different thickness as shows in Figure 3, this Figure shows the effect of change the

between 900 ^{o}C and 400 ^{o}C in which chrominium-rich carbide can be formed depending on the duration, i.e. scanning velocity and number of passes, and in addition, significant deformation due to thermal stress is also involved in HAZ (II). Scanning Electron Micrographs (SEM) analysis as recorded in figure 4 to investigation of laser-bent zone of specimen 304 Stain Steel Graphite coating at magnification (Inconel) X800 after exposure to etched by oxalic acid 10% are identified as (a) general appearance-cross section, (b) melted

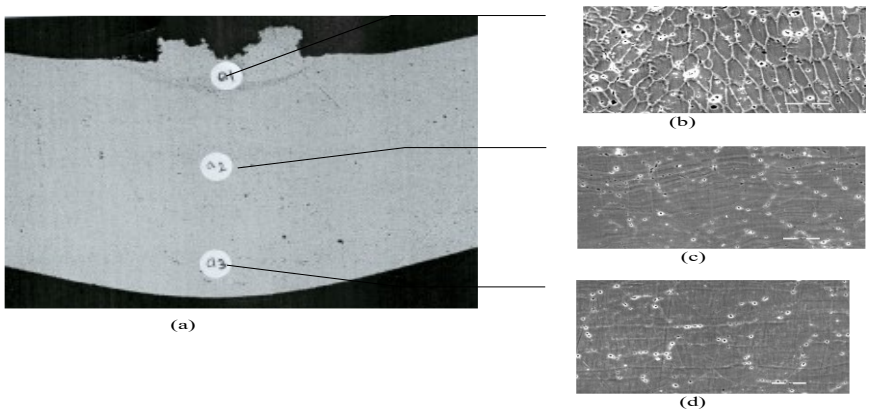

Figure 4. (a, b, c, d). SEM micrographs of laser-bent zone of Specimen 304 S.S. (a): general appearance-cross section, (b): melted zone,(c): HAZ (I) and (d): HAZ (II).

https://doi.org/10.61856/wb55x818

zone, (c) HAZ (I) and (d) HAZ (II). Figure 4a shows atypical cross section of laser-bent specimens, with melting occurred on the irradiated surface. The melt depth increased with increase in number of passes. From the microstructural observation from figure 4b, it was revealed that the melt zone contained solidified dendritic structure with dendritic arm space. Immediately after the solid-liquid interface, grain-coarsening region, formed due to heating effect from the top surface, was found in HAZ (I) as shows in figure 4c, while no significant change in grain size was found in HAZ (II) (figure 4d) though deformation, i.e. slightly elongated grains, due to thermal stress was present. When melting did not occur, only HAZ (I) and HAZ (II) were present.

3.2.2 Hardness profiles

The corrosion behaviour was further determined by the DL-EPR in de-aerated 0.5M H_2SO_4 +0.01M KSCN, and scanning rate of 1.67 mV/s using Salortron 1280, potentiostat and a conventional three-electrode cell

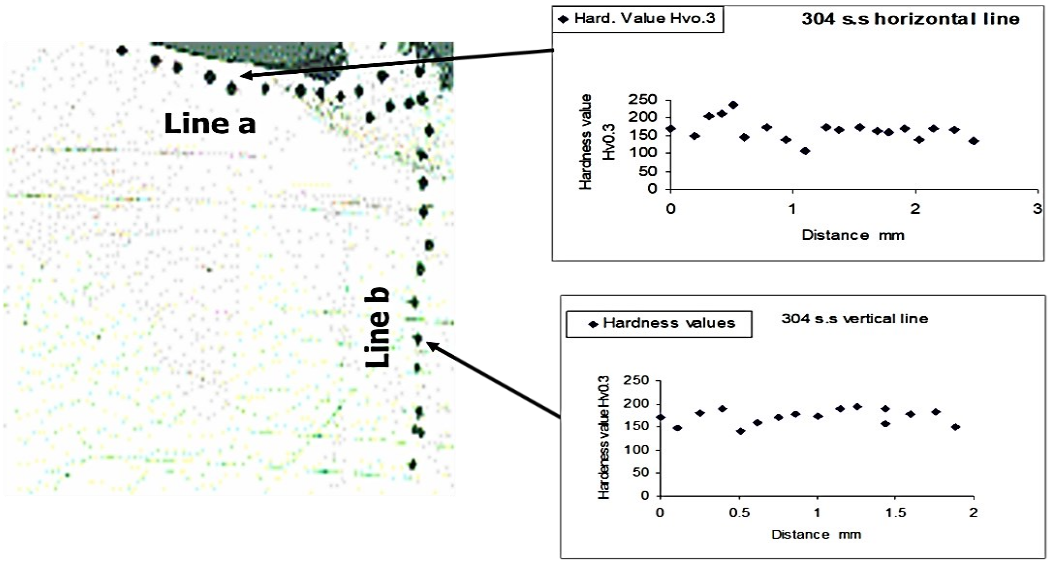

Figure 5. 304-g-3-smallest angle lines a and b

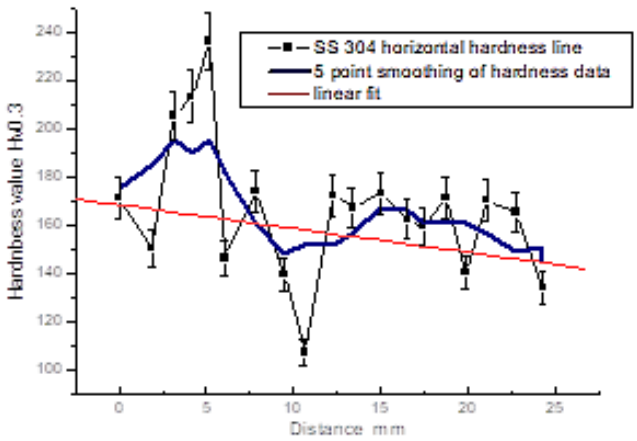

Figure 5 (a). 304-g-3-smallest angle line a

https://doi.org/10.61856/wb55x818

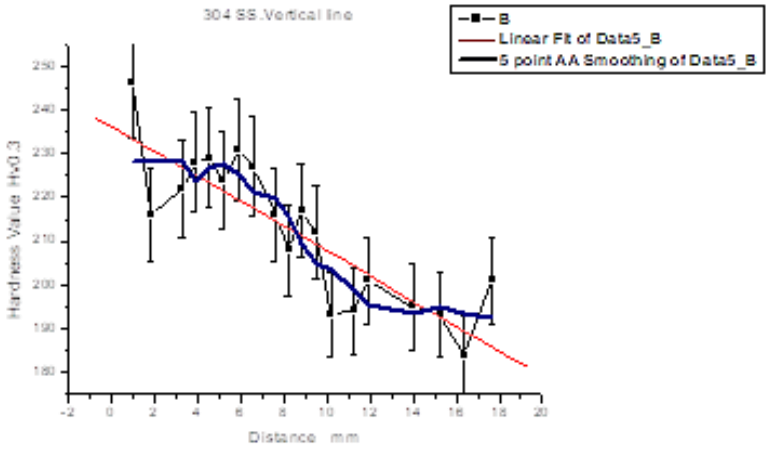

Figure 5 (b1). 304-g-3-line b

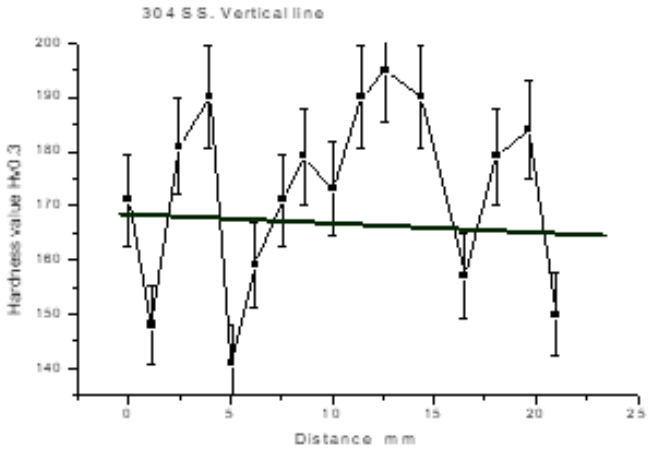

Figure 5 (b2). 304-g-8-line b

employing a Pt counter electrode and saturated calomel reference electrode (SCE). Freshly polished surfaces to 1200 grit with emery paper and 3 mm diamond paste in order to present a uniform surface roughness were immersed in the electrolyte for 30 min to determine the corrosion potential (Ecorr). After establishing the Ecorr, for 304 stainless steels, the specimen was polarised from the initial potential of 50 MV (vs.Ecorr) in the cathodic region to a version potential (Erev) of + 250mV (vs.SCE)in the passive region .As soon as this potential was reached, the scanning direction was reversed and potential was degreased to -in terms of degree of sensitisation, was characterised by the reactivation ratio, Qr/Qp (t, T), where Qr (c/m^2 is the reactivation and Qp (C/m^2) is the activation–passivation surface charge density. The Micro-hardness profiles across the thickness of the specimen 304 austenitic S.S Variation in average Vickers hardness profiles across the thickness of the specimen 304 austenitic S.S shows in figure 5, as measured (line a) from the centre of MZ of the laser treated near the top surface to the untreated zone of sample 304-g-3, and (line b) from the centre of MZ of the laser treated to the sample 304-g-8 bottom as shown in figure 5 (b1 and b2 for 2 different samples of 3-g and 8-g).

3.4 Establishment of laser processing windows

3.4.1 EPR test analysis

https://doi.org/10.61856/wb55x818

The good interpretation of the EPR test necessitates studying not only the evolutions of Qr/Qp values but also the evolutions of the separate Qr and Qp values. And current peak is also an important parameter to evaluate the performance of intergranular corrosion of stainless steel. Larger reaction peak and Qr/Qp corresponds to more sensitized specimen. From figure 6 (a, b) EPR 304 S.S results of both samples are represented. These samples include initial received samples as well as the same samples after laser binding in order to compare them. Table 1 shows Ecorr shift negative after laser bending. The laser bended specimen presents a larger reactivation current than as-received specimen. And it has larger Qr/Qp and Ir/Ip. It shows the former is prone to be attack by intergranular corrosion.

Table 3: Recorded EPR results of 304 S.S of both samples as received and the same sample after laser binding to compare.

Specimen	E_{corr},V (vs.SCE)	Qr (C/cm^2)	Qp (C/cm^2)	Ir (mA)	Ip (mA)	Qr/Qp (%)	I_r/I_p (%)
As received	-0.4251	0.1091	4.0838	2.15	75.93	2.67	2.83
Laser-bent 304 S.S	-0.4379	0.3865	6.3772	4.46	88.19	6.06	5.06

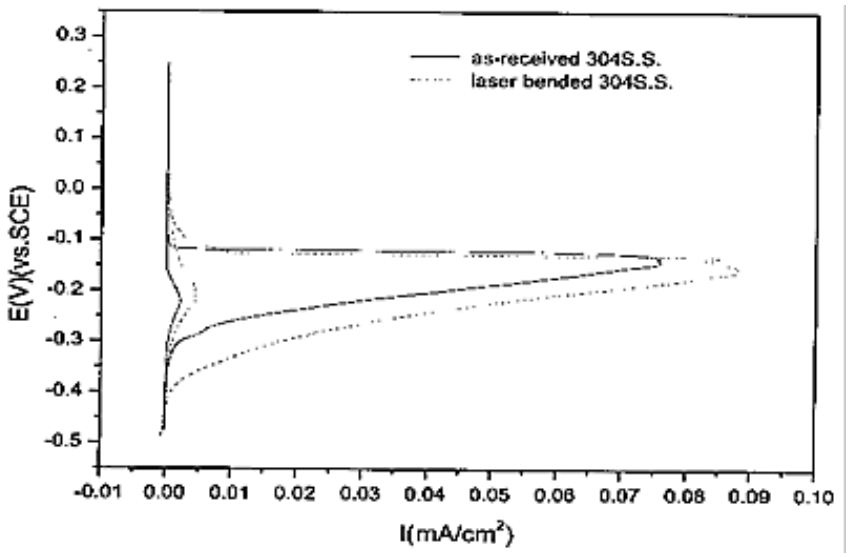

Figure 6. Shows EPR results of 304 S.S of both samples as received.

3.3 Corrosion studies

The etched structures were classified into the following types: step structure (steps only between grains, no ditches at grain boundaries), ditch structure (one or more grains completely surrounded by ditches) and Dual structure (some ditches at grain boundaries, but no single grain completely surrounded by ditches.

4. Conclusions

In this work, laser bending of 304 austenitic only has been investigated in terms of bending angle, microstructure, microhardness and corrosion performance within bent-zone and HAZs. The following conclusions are drawn:

1. Bending angle was found to vary from 6.5°-29.5° 304 stainless steel and 7°-19.5° for 430 stainless steel and increased with decrease in scanning velocity and increase in number of passes.
2. Maximum bending angle of 29.5° for 304 stainless steel can be achieved without surface melting; however, when larger bending angles are required, surface melting is inevitable.
3. The microstructure of the bent zone consisted of melt zone with significantly refined dendritic structure and followed by HAZ (I) with coarsened grains and then by HAZ (II) with pronounced grain elongation.

https://doi.org/10.61856/wb55x818

4. The microhardness Variation in average Vickers hardness profiles across the thickness of the specimen hardness as measured (a) from the centre of MZ of the laser treated near the top surface to the untreated zone; (b) from the centre of MZ of the laser treated to the sample bottom. The dependence of the hardness changes on the material and the sheet thickness. A decrease of the hardness occurs until the hardness reaches the value of the base material temperature. The melt depth increased with increase in number of passes and hardness decreases with increasing depth, then hardness decreases with increase in number of passes (N) [5] No sign of corrosion was found in melt zone and HAZ (I), but intergranular corrosion was revealed in HAZ (II) for 304 stainless when bending angle was greater than 29.5°; due to the sensitisation created by the repeat of laser scans.

5. Outcome and future work

Up to this period, this research completed for the recent developments in the area of material science, material laser treatment and 304 and 340 Stainless steel alloys. And for part B of this work, the investigation result for 430 stainless steels when bending angle was greater than 19.5° were observed due to the sensitisation created by the repeat of laser scans and more, using the same analysis tool, then recorded in part B of this work.

6. Acknowledgements

I wish to thank my supervisors, prof. Liu Zhou and Prof Peter Skeldon for their support at Manchester university, UK, and Manchester university academic staff for their collaboration and advice.

7. References

B.S. Yilbas, Akhtar, S. S., & Karatas, C. (2012). Laser bending of AISI 304 steel sheets: Thermal stress analysis. Optics & Laser Technology, 44(4), 1314-1322. 10.1016/j.optlastec.2011.06.021

B.S. Yilbas, Akhtar, S. S., & Karatas, C. (2014). Laser bending of metal sheet and thermal stress analysis. Optics & Laser Technology, 60, 46-54. 10.1016/j.optlastec.2013.12.023

Yan, C., Hao, L., Hussein, A., & Raymont, D. (2012). International Journal of Machine Tools & Manufacture Evaluations of cellular lattice structures manufactured using selective laser melting. *International Journal of Machine Tools and Manufacture*, *62*, 32–38. Retrieved http://linkinghub.elsevier.com/retrieve/pii/

F. Quadrini, Santo, L., & Trovalusci, F. (2010). Laser forming of open-cell aluminium foams. Journal of Materials Processing Technology, 210(15), 2053-2060. https://doi.org/10.1016/j.jmatprotec.2010.04.010

H. Shen, Cheng, J., & Hu, H. (2006). An analytical formula for estimating deformation in laser forming. Computational Materials Science, 37(3), 293-299. Dl.

H. Shen, Cheng, J., & Hu, H. (2010). Experimental study on negative laser bending process of steel foils. Optics & Laser Engineering, 48(5), 628-635. DL.

Yongjun Shi,Yancong Liu,Peng Yi,Jun Hu (2012). Effect of different heating methods on deformation of metal plate under upsetting mechanism in laser forming. Optics & Laser Technology, 44(2), 486-491 https://doi.org/10.1016/j.optlastec.2011.08.019

Manna, A. K., Nath, A. K., & Dutta Majumdar, J. (n.d.). Laser bending characteristics of AISI 304 stainless steel. Department of Materials Engineering, Indian Institute of Technology, Kharagpur, India.DL.

Hennige, T. (2000). Development of irradiation strategies for 3D-laser forming. Journal of Materials Processing Technology, 103(3), 364-369.DL.

Zhang, X.R., & Xu, X. (2004). Study on the laser forming process. Journal of Applied Mechanics, 71(3), 321-328. DL.

Shi, Y., Liu, J., & Wu, D. (1998). Laser bending of leadframe materials. Journal of Materials Processing Technology, 84(1-3), 164-169. DL.

Shi, Y., Wu, D., & Liu, J. (2014). An experimental investigation of underwater pulsed laser forming. Optics & Laser Engineering, 55, 11-19. DL.